

Stellar Evolution onto and off the Main Sequence

$$X = 0.708, Y = 0.272, Z = 0.020$$

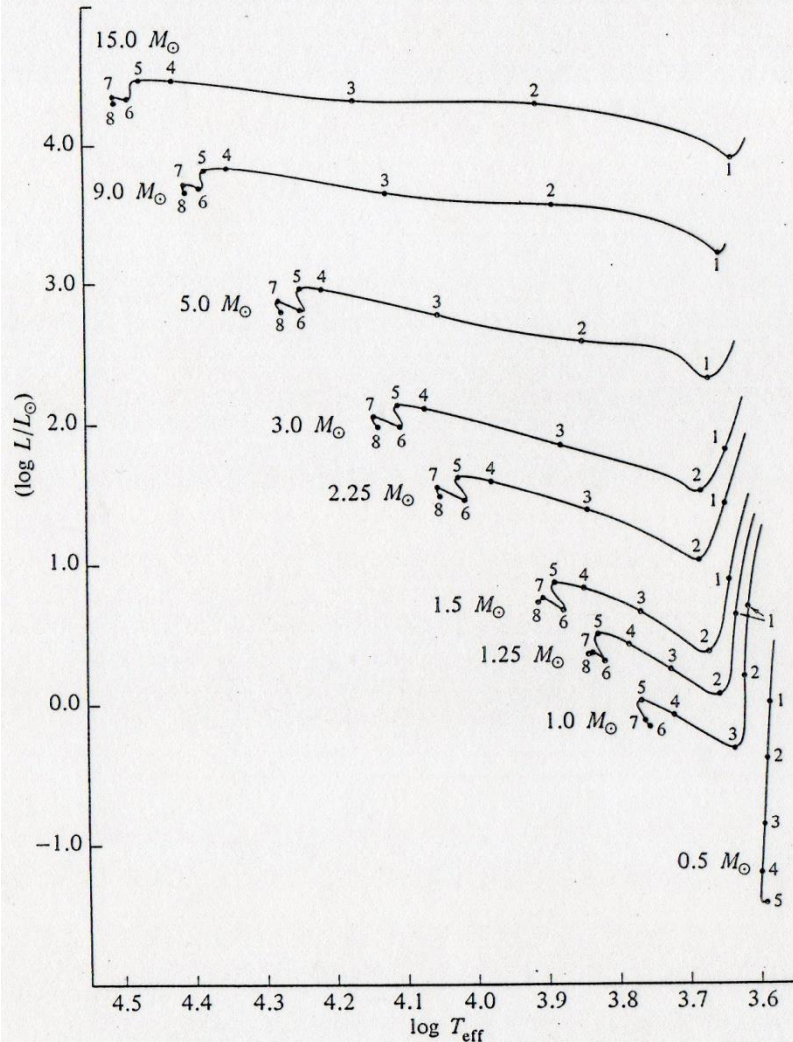


Fig. 7-3A Evolutionary Tracks of Pre-Main-Sequence Stars in the Hertzsprung-Russell Diagram. The mass, in units of the solar mass, is given at the left of each track. The small numbers correspond to the points in Table 7-4A, which give the time measured from the initial model for each mass. The units of T_{eff} are degrees Kelvin. [After I. Iben, Jr., 1965 (321).] **ApJ 141, 993**

Table 7-4A Time t in Years Measured from the Initial Model for Each Mass. The last point for each mass represents the main sequence.* [From I. Iben, Jr., 1965 (321).]

POINT IN FIG. 7-3A	MASS OF MODEL (UNITS OF THE SOLAR MASS)								
	15	9	5	3	2.25	1.5	1.25	1.0	0.5
	10^4	10^5	10^5	10^6	10^6	10^7	10^7	10^7	10^8
1	0.067	0.014	0.294	0.034	0.079	0.023	0.045	0.012	0.003
2	0.377	0.015	1.069	0.208	0.594	0.236	0.396	0.106	0.018
3	0.935	0.364	2.001	0.763	1.883	0.580	0.880	0.891	0.087
4	2.203	0.699	2.860	1.135	2.505	0.758	1.115	1.821	0.309
5	2.657	0.792	3.137	1.250	2.818	0.862	1.404	2.529	1.550
6	3.984	1.019	3.880	1.465	3.319	1.043	1.755	3.418	—
7	4.585	1.915	4.559	1.741	3.993	1.339	2.796	5.016	—
8	6.170	1.505	5.759	2.514	5.855	1.821	2.954	—	—

* Each entry must be multiplied by 10^6 as given at the head of each column.

Table 7-4B The Logarithm of the Time in Seconds, $\log t$, Measured From the Initial Models for Masses $1 M_{\odot}$ and $15 M_{\odot}$. [From data of I. Iben, Jr., 1965 (321).]

POINT IN FIG. 7-3A	MASS OF MODEL (UNITS OF THE SOLAR MASS)	
	15	1.0
1	10.33	12.57
2	11.07	13.52
3	11.47	14.45
4	11.84	14.76
5	11.92	14.90
6	12.10	15.03
7	12.16	15.20
8	12.29	—

"Kinks"

$$\log \tau \approx 14.5$$

$$\log \tau \approx 15.0$$

"Introduction to Stellar Atmospheres and Interiors" by Eva Novotny

STELLAR EVOLUTION. I. THE APPROACH TO THE MAIN SEQUENCE*

ICKO IBEN, JR.

California Institute of Technology, Pasadena, California

Received August 18, 1964; revised November 23, 1964

ABSTRACT

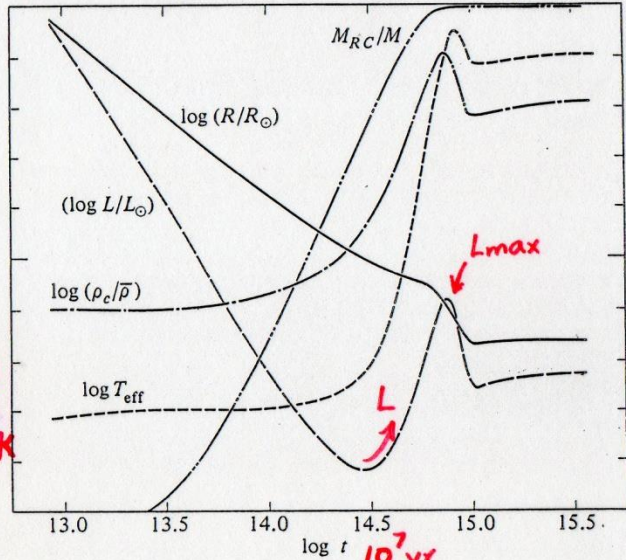
The manner in which nuclear reactions replace gravitational contraction as the major source of stellar luminosity is investigated for model stars of population I composition in the mass range $0.5 < M/M_{\odot} < 150$. By following in detail the depletion of C^{12} from high initial values down to values corresponding to equilibrium with N^{14} in the C-N cycle, the approach to the main sequence in the Hertzsprung-Russell diagram and the time to reach the main sequence, for stars with $M \geq 1.25 M_{\odot}$, are found to differ significantly from data reported previously.

PMS

1 M_{\odot}

$$L \equiv L_{\text{nuc}} + L_{\text{grav}}$$

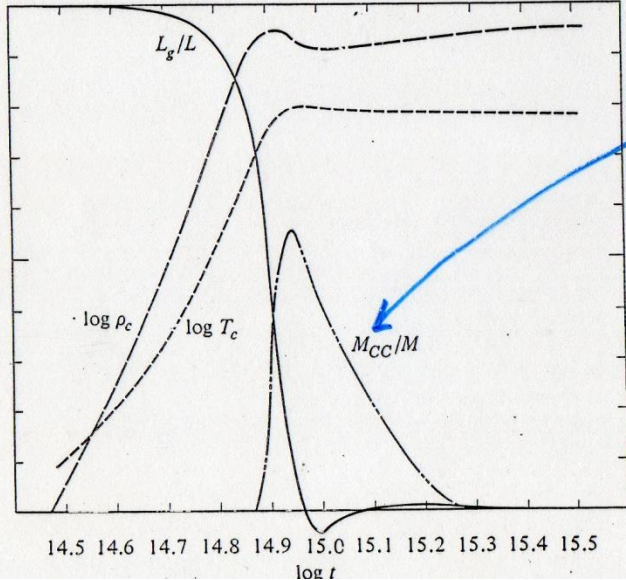
M_{RC}/M	$\log(R/R_{\odot})$	$\log(\rho_c/\bar{\rho})$	$\log T_{\text{eff}}$	$\log(L/L_{\odot})$
1.0	+0.6	2.0	3.78	+0.6
0	-0.4	0	3.58	-0.4



$\log T_{\text{eff}} \sim 3.62$
 $T_{\text{eff}} \sim 4200\text{K}$

$\tau \sim 14.5$
 $L \uparrow$
 \therefore nuclear reactions
 $H^1 \rightarrow H^2 \rightarrow He^3$
 $C^{12} \rightarrow N^{13} \rightarrow C^{13} \rightarrow N^{14}$
 σ_b
 Rest reactions do not operate
 \Rightarrow temporary

M_{CC}/M	$\log \rho_c$	$\log T_c$	L_g/L
0.20	2.0	7.25	1.0
0	1.0	6.75	0



\Rightarrow convective core until C^{12} depleted (p-p chain more important)

$$L_{\text{nuc}} = \int_0^M \epsilon dM_r$$

r	P	ρ	T	L_r
$0.882 R_{\odot}$	1.647×10^{17}	85.59	14.07×10^6	$0.911 L_{\odot}$
0	0	0	0	0

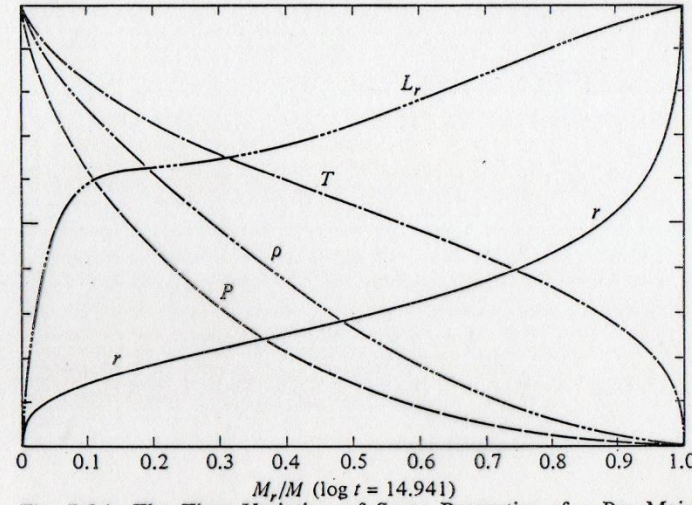


Fig. 7-5A The Time Variation of Some Properties of a Pre-Main-Sequence Star of Mass $1 M_{\odot}$. The abscissa is $\log t$, where t is the time in seconds measured from the initial model of the series for this mass. The upper and lower limits of each ordinate are given. The ordinates are: M_{RC}/M , the fraction of the total mass contained in a radiative core; $\log(R/R_{\odot})$, where R/R_{\odot} is the total radius relative to that of the Sun ($R_{\odot} = 6.96 \times 10^{10}$ cm); $\log(\rho_c/\bar{\rho})$, where ρ_c is the central density and $\bar{\rho}$ is the mean density; $\log T_{\text{eff}}$, where T_{eff} is the effective temperature in degrees Kelvin; and $\log(L/L_{\odot})$, where L/L_{\odot} is the luminosity relative to that of the Sun ($L_{\odot} = 3.86 \times 10^{33}$ erg sec $^{-1}$). [After I. Iben, Jr., 1965 (321).]

Fig. 7-5B The Time Variation of Some Properties of a Pre-Main-Sequence Star of Mass $1 M_{\odot}$. The abscissa is $\log t$, where t is the time in seconds measured from the initial model of the series for this mass. The upper and lower limits of the scale for each curve are given. The ordinates are M_{CC}/M , the fraction of the mass contained in a convective core; $\log \rho_c$, where ρ_c is the central density in gm cm $^{-3}$; $\log T_c$, where T_c is the central temperature in degrees Kelvin; and L_g/L , the net fraction of the luminosity that is generated by gravitational contraction (but not necessarily the fraction of the emitted radiation that is due to gravitational contraction—see text). The value of L_g/L becomes negative near $\log t = 15.0$: zero for this ordinate is on the horizontal axis. [Adapted from I. Iben, Jr., 1965 (321).]

Fig. 7-5C A Model of Mass $1 M_{\odot}$ During the Pre-Main-Sequence Phase at Time $\log t = 14.941$. The time is measured in seconds from the initial model of the series for this mass. The abscissa is the fractional mass M_r/M . The upper and lower limits of each ordinate are given. Each upper limit is the maximum value in the model. The ordinates are r , the radius in units of the solar radius ($R_{\odot} = 6.96 \times 10^{10}$ cm); P , the pressure in dyne cm $^{-2}$; ρ , the density in gm cm $^{-3}$; T , the temperature in degrees Kelvin; and L_r , the net luminosity in units of the solar luminosity ($L_{\odot} = 3.86 \times 10^{33}$ erg sec $^{-1}$). [Adapted from I. Iben, Jr., 1965 (321).]

Pre-main Sequence Evolution of a 1 M_⊙ star

$$\tau < 2 \times 10^{14} \text{ s (i.e., } 7 \times 10^6 \text{ yr)}$$

$$T_{\text{eff}} \sim \text{const} \sim 4200 \text{ K} \quad R \downarrow \Rightarrow L \downarrow$$

due to ionization of H & He
a deep convective envelope

$$\rho_c / \bar{\rho} \sim \text{const} \quad (\text{Hayashi track})$$

Star completely convective in
the first 10^6 yr

L_g/L : energy from gravitational contraction

$\tau \sim 14.5$, $L \uparrow$ \Rightarrow nuclear reactions
(10^7 yr)

(cont.)

~ 15

\Rightarrow expanding the core

$\rho_c \downarrow$, $T_c \downarrow$

But T_c not high enough

only ${}^1\text{H} \rightarrow {}^2\text{D} \rightarrow {}^3\text{He}$

${}^{12}\text{C} \rightarrow {}^{13}\text{N} \rightarrow {}^{13}\text{C} \rightarrow {}^{14}\text{N}$

The rest of PP chains or CNO cycle do not operate yet

Note

$$L_{\text{nc}} + L_g \equiv L$$

$\tau \sim 15$, $L_g < 0$ (\because core expansion)

$$\epsilon_{\text{nuc}} \uparrow \rightarrow \nabla T \uparrow$$

\Rightarrow A temporary convective core ($\tau \sim 14.9$)
until ^{12}C is depleted and
pp chains become important

Eventually $\nabla T \downarrow$ at core, convective core \downarrow
($\tau \sim 15.3$)

$\tau \sim 15$, $L \rightarrow L_{\text{max}}$

Structure of star adjusts

∴ Energy sources from gravitational
to nuclear processes

⇒ ^{12}C main sequence ! Point 5

short lasting, depletion rapidly

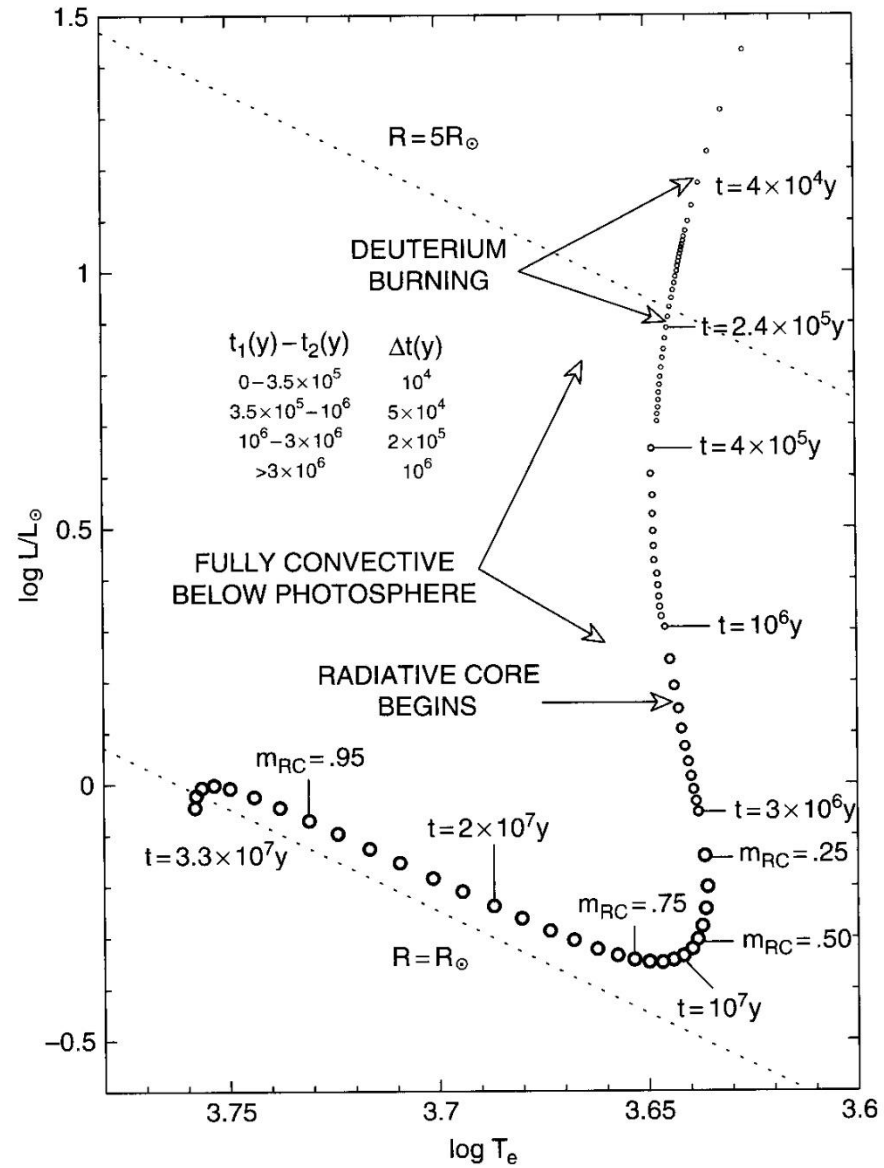
→ slight contraction

T_c, ρ_c high enough for PP reactions

to be the sole energy source.

For all Stars $M \gtrsim M_{\odot} \Rightarrow$ convective core
 ^{12}C burning \longrightarrow recedes
 \downarrow

For Stars $M \gtrsim 1.25 M_{\odot} \Rightarrow$ double luminosity
maxima and minima



Pre main sequence evolution in the HR diagram of a low mass model ($M = 1M_{\odot}, Z = 0.01, Y = 0.25$)

For $0.5 M_{\odot}$ stars,

ρ_c, T_c not high enough for ^{12}C
burning

For $M \lesssim 0.1 M_{\odot}$ (dependent of μ)

T_c not high enough for even H
burning

\Rightarrow contraction continues

\rightarrow degenerate core

\Rightarrow black dwarfs

... nowadays called **brown dwarfs**

only the initial, nearly vertical descent

$\therefore T_c, P_c$ never high enough to ignite ^{12}C

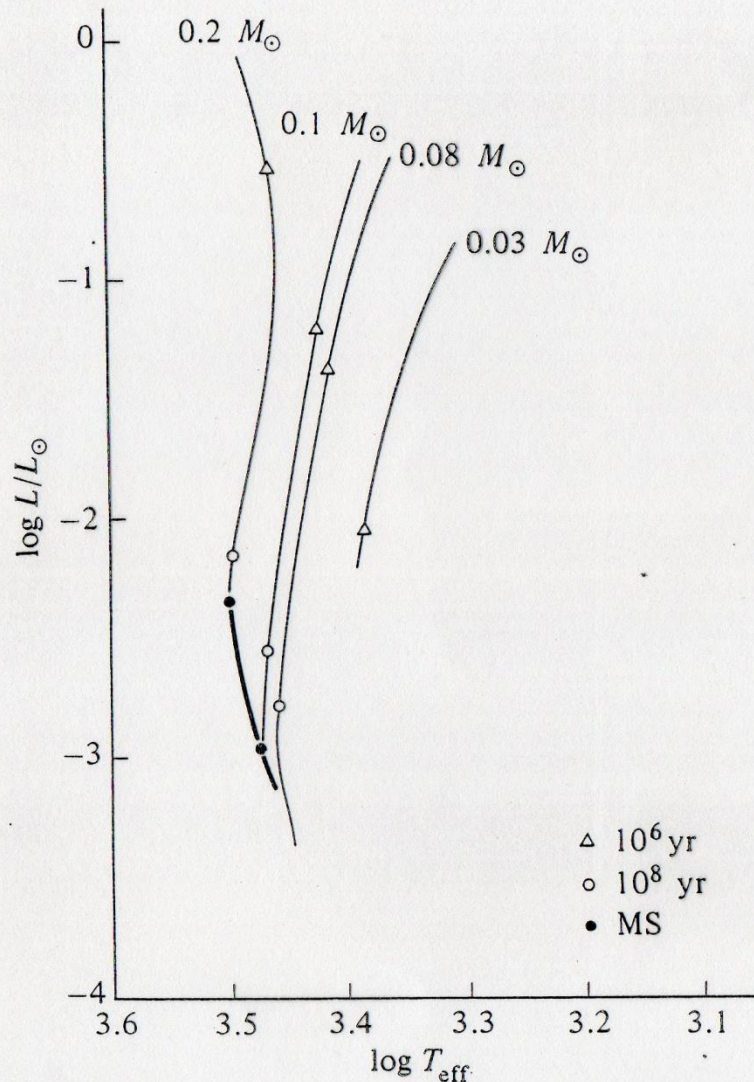


Fig. 7-3B Evolutionary Tracks of Pre-Main-Sequence Stars of Low Mass in the Hertzsprung-Russell Diagram. The masses, and the ages at two points on each track, are indicated. The heavy curve (MS) is the hydrogen-burning main sequence. The convective parameter is assumed to have the value $l/H = 1.0$. [Adapted from A. S. Grossman and H. C. Graboske, Jr., 1971 (400).]

Rotation → star cooler and fainter

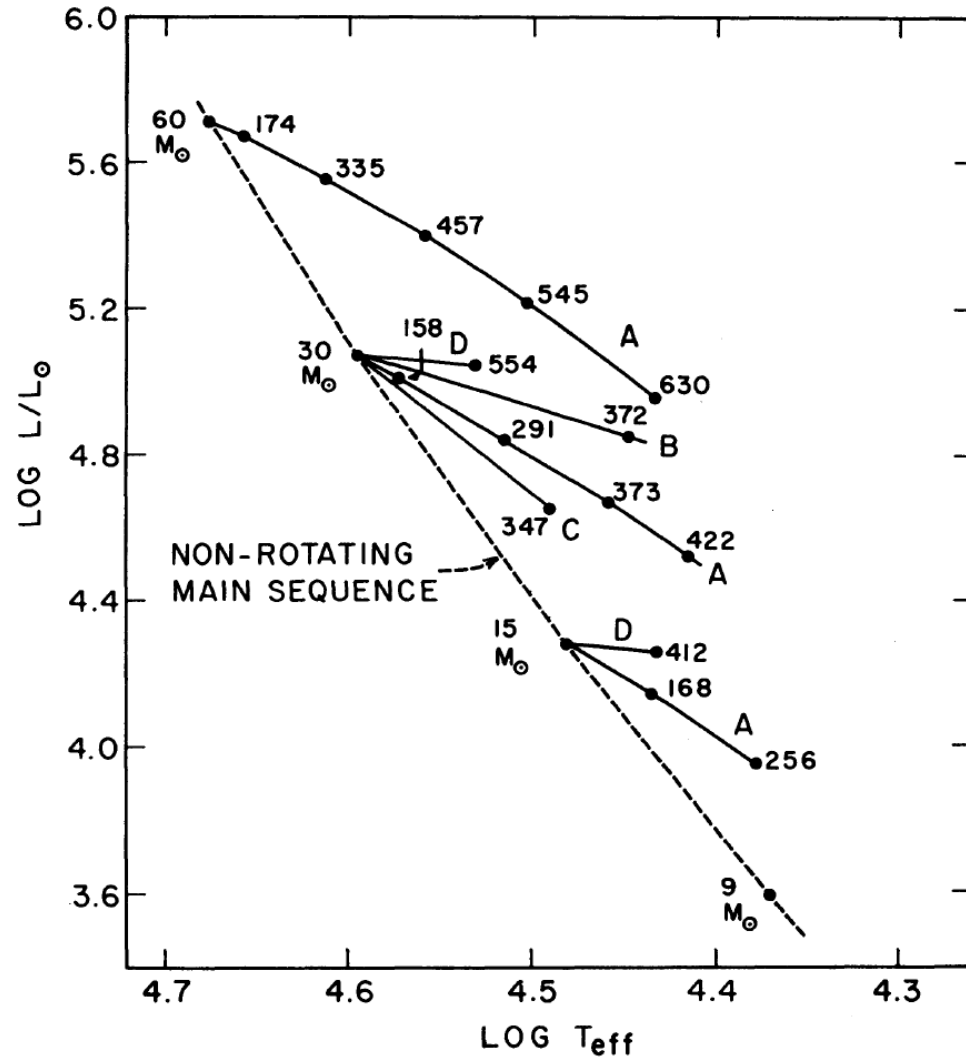


FIG. 2.—Theoretical H-R diagram showing model sequences of increasing angular momentum (*solid curves*). Numbers on curves give calculated velocities at the equator in km sec^{-1} . The distribution of angular momentum for each sequence is indicated by the letter A, B, C, or D.

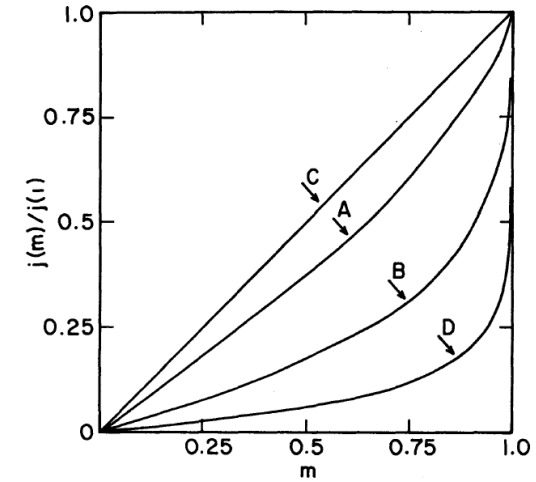


FIG. 1.—Angular momentum per unit mass, as a function of mass fraction interior to a given cylinder about the axis of rotation, for three assumed laws of differential rotation (Cases A, B, and C) and for a uniformly rotating model (Case D) of $30 M_{\odot}$, $\log J = 52.73$.

D: solid body rotation

Rotation law:

angular momentum distribution $j(m_w)$ as a function of, m_w , the mass fraction interior to the cylinder of radius w about the rotation axis.

Rotation

→ line broadening
and shallowing

HR 9024 (OU And)
G1 IIIe

HR 3664 G6 III

Line blending

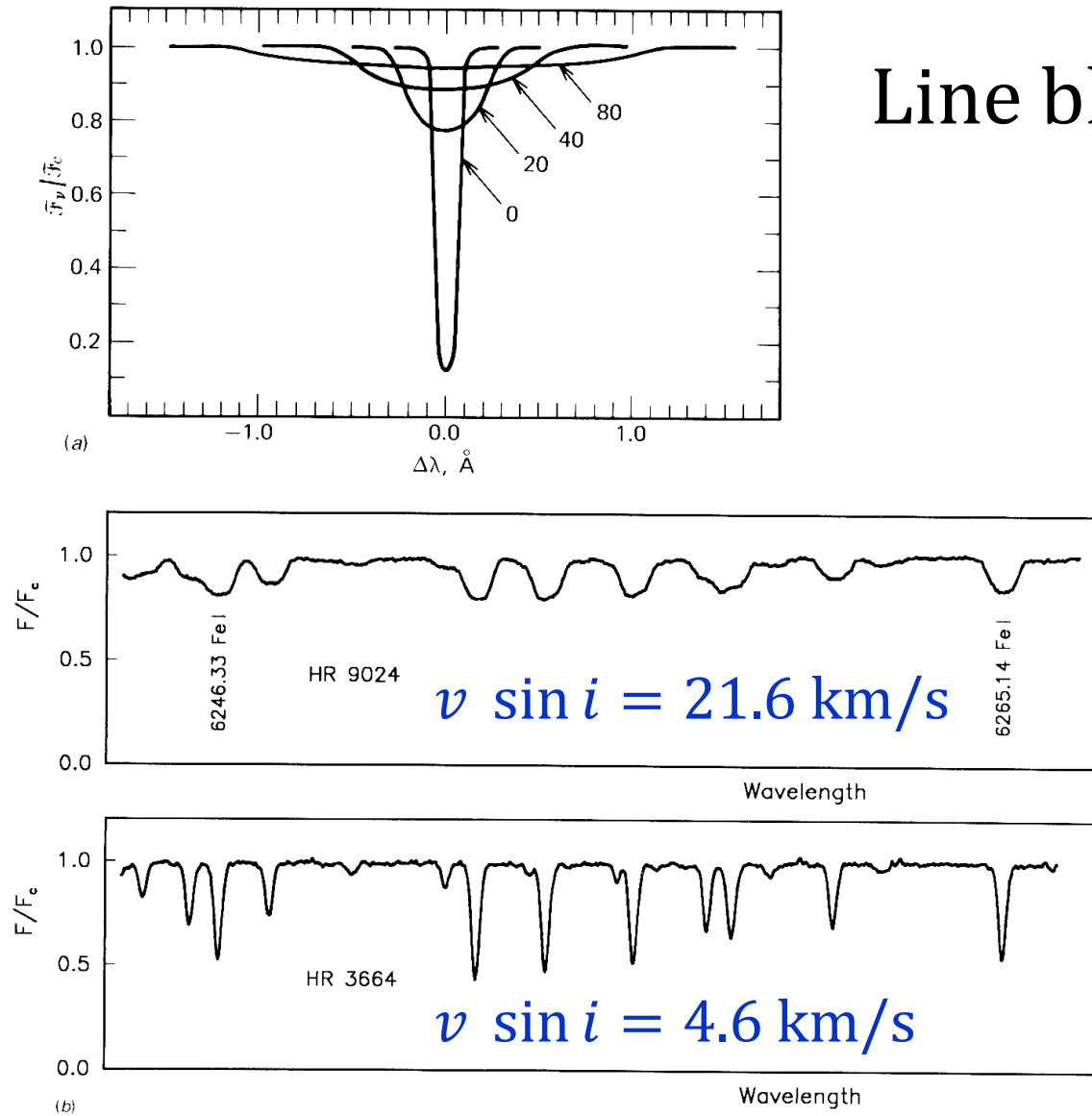


Fig. 17.7. (a) Computed profiles illustrate the broadening effect of rotation. The profiles are labeled with $v \sin i$. the wavelength is 4243 Å, and the line has an equivalent width of 100 mÅ. (b) These two early-G giants illustrate the Doppler broadening of the line profiles by rotation.

Gray p. 376

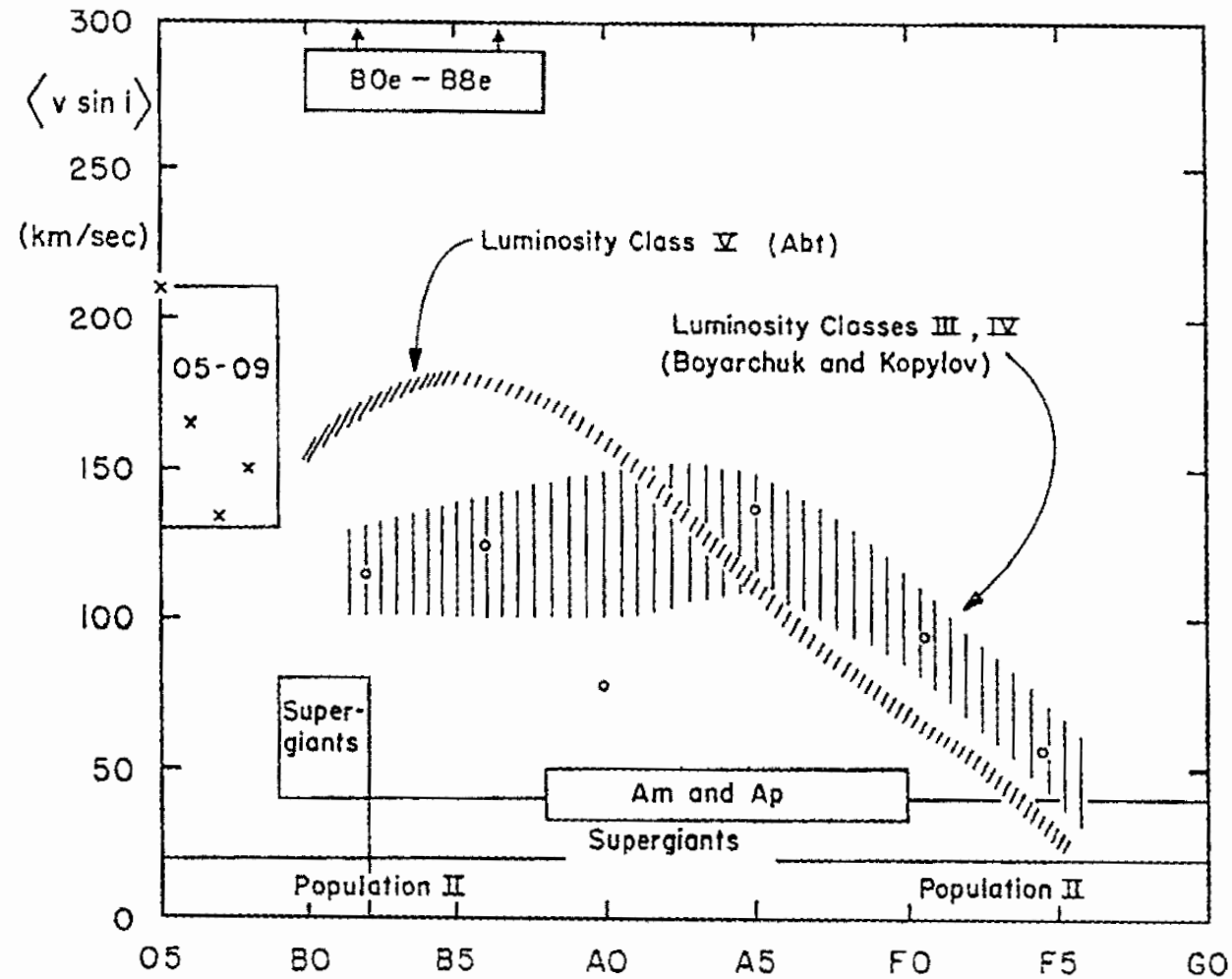


Fig. 3. Projected equatorial velocities, averaged over all possible inclinations, as a function of spectral type. On the main sequence (luminosity class V), early-type stars have rotational velocities that reach and even exceed 200 km/s; these velocities drop to a few km/s for late-type stars, such as the Sun (type G2) (Slettebak [20]; courtesy Gordon & Breach)

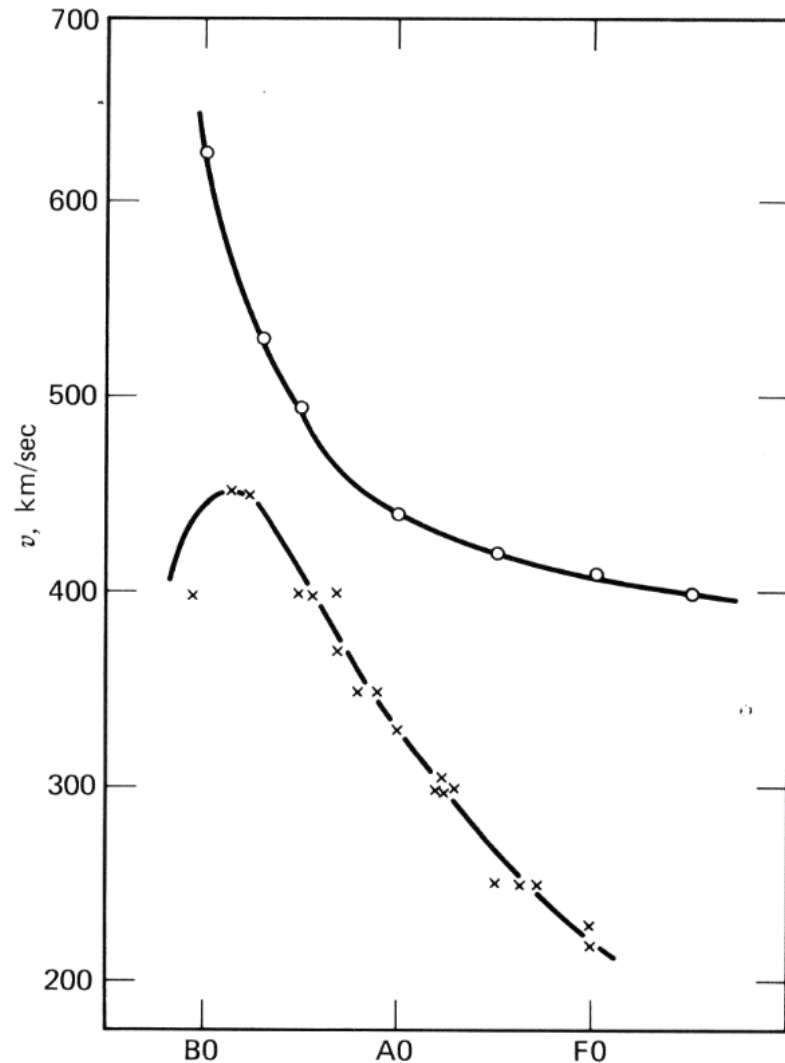


Fig. 17.22. The fastest rotation rates are shown by the \times s. The theoretical break-up velocities (top curve) approach the observed relation most closely in the B-star range. (Data from Slettebak (1966).)

- ✓ The fastest single rotators, other than remnant objects such as neutron stars, are Be stars.
- ✓ As fast as ~ 450 km/s, close to break-up speed
- ✓ Mass loss preferentially along the equators.
- ✓ Stars no longer spherical

Rotation vs Spectral Type

- ✓ Massive stars are fast rotators.
- ✓ Rotation declines in the F type (convection? disk?)
- ✓ Low-mass stars spin down quickly early on (disk-star coupling of **B** field), and then experience weak-breaking on the MS due to magnetic breaking and winds

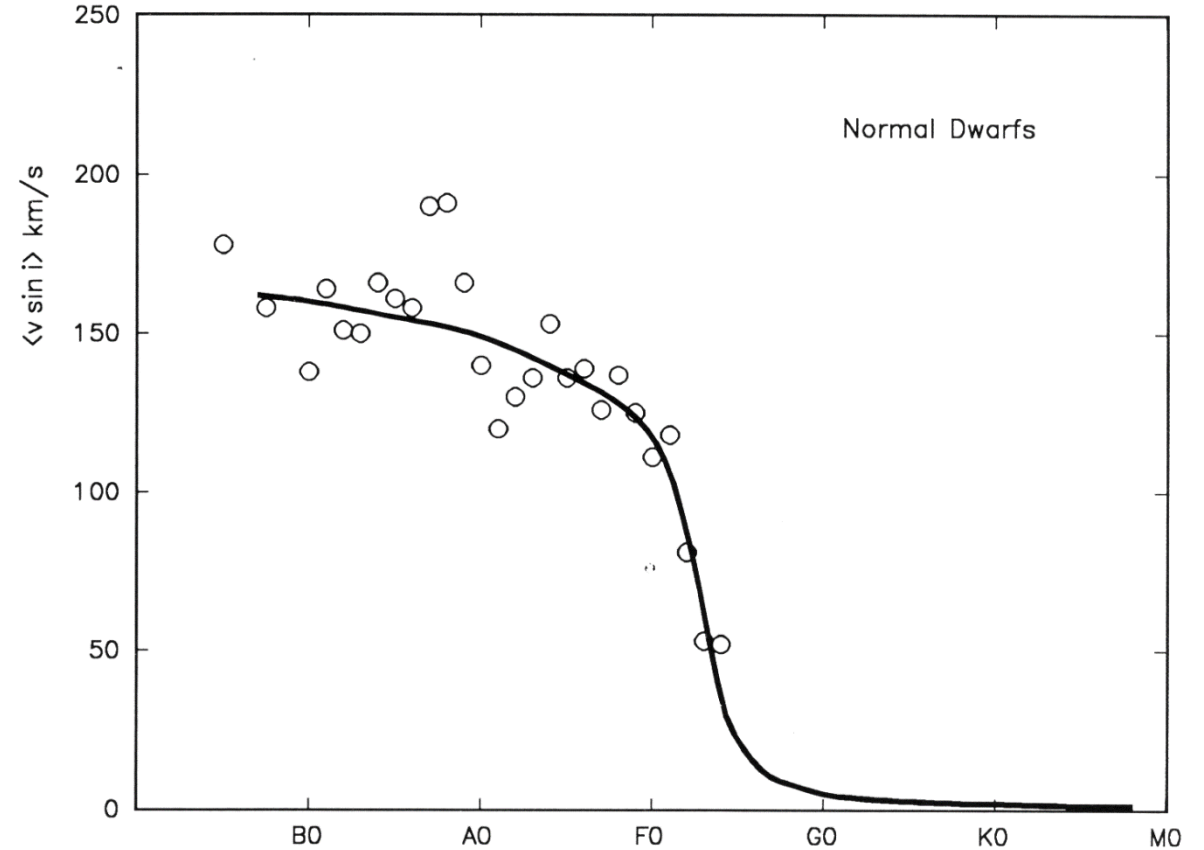


Fig. 17.16. The average rotation rates are shown for spectral intervals as a function of spectral type. (Data are from Uesugi and Fukuda (1982), Soderblom (1983), and Gray (1982b, 1984b).)

- ✓ Giants and supergiants rotate slowly because of angular momentum conservation.

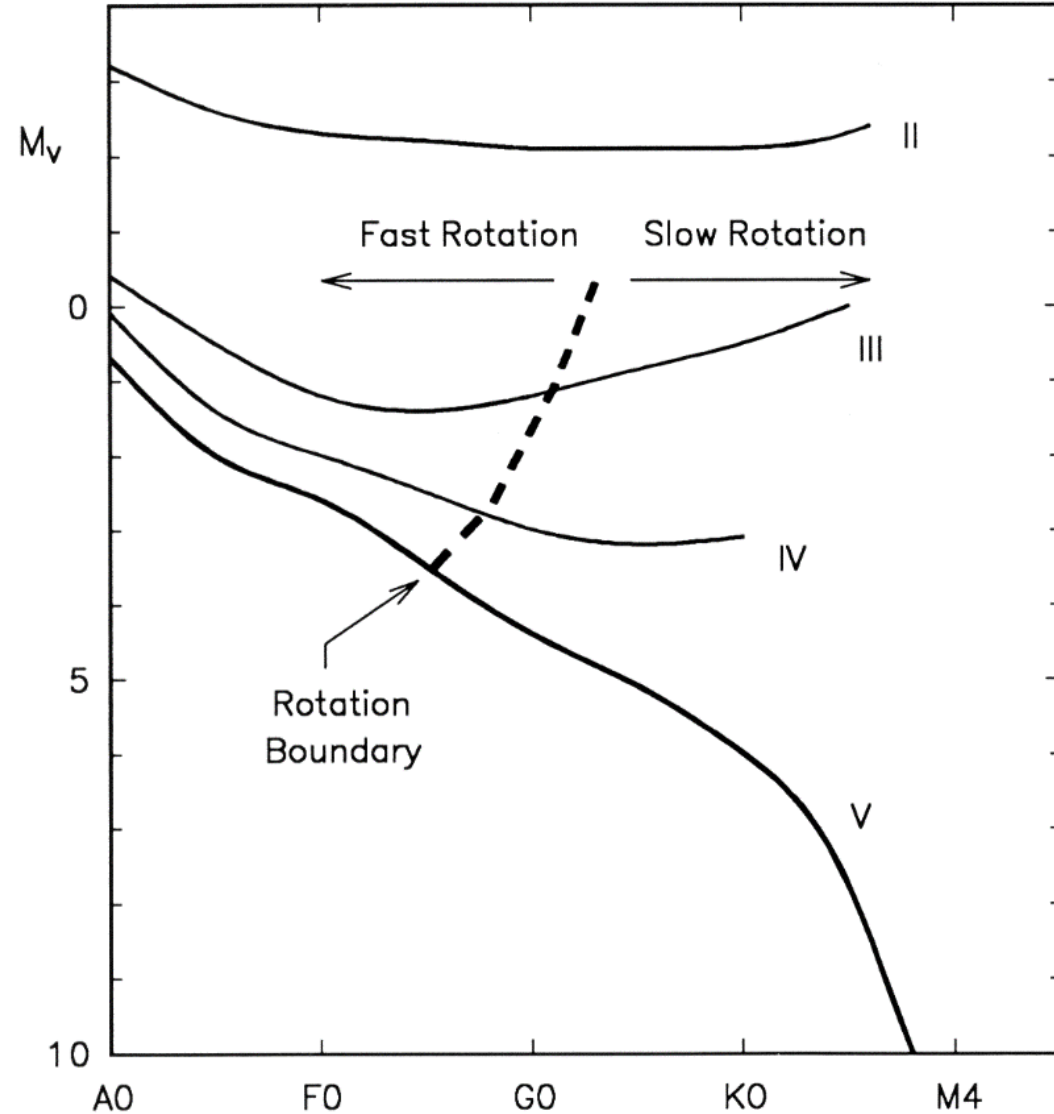
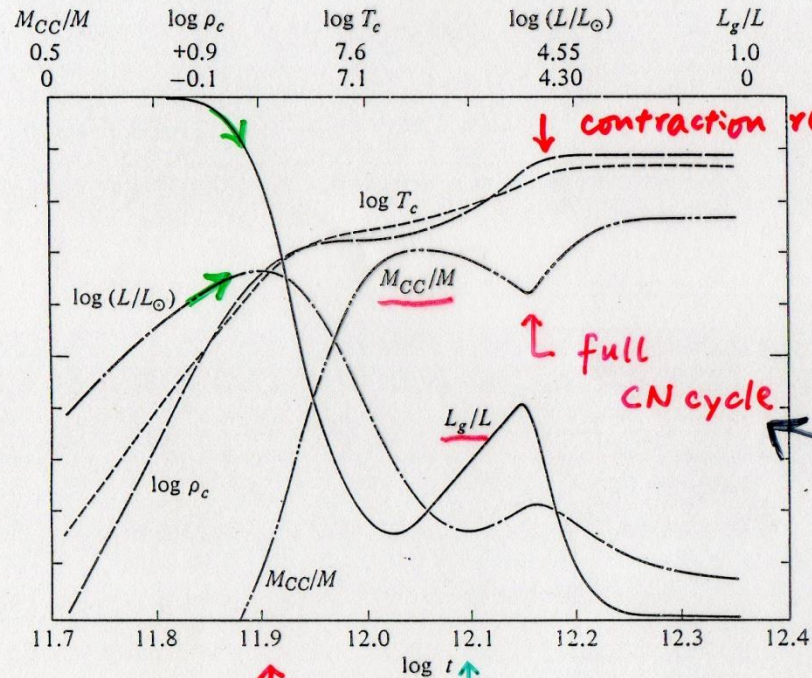


Fig. 17.21. The rotation boundary separates fast rotation from slow rotation.

PMS

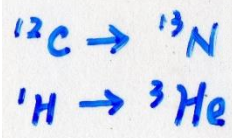
$15 M_{\odot}$

Fig. 7-6 The Time Variation of Some Properties of a pre-main-sequence Star of Mass $15 M_{\odot}$. The abscissa is $\log t$, where t is the time in seconds measured from the initial model of the series for this mass. The upper and lower limits of each ordinate are given. The ordinates are M_{CC}/M , the fraction of the total mass contained in a convective core; $\log \rho_c$, where ρ_c is the central density in gm cm^{-3} ; $\log T_c$, where T_c is the central temperature in degrees Kelvin; $\log (L/L_{\odot})$, where L/L_{\odot} is the luminosity relative to the solar luminosity ($L_{\odot} = 3.86 \times 10^{33}$ erg sec^{-1}); and L_g/L , the net fraction of the luminosity that is generated by gravitational contraction (but not necessarily the fraction of the emitted radiation that is due to gravitational contraction—see text). [Adapted from I. Iben, Jr., 1965 (321).]



$\epsilon_{\text{grav}} \downarrow$ $\epsilon_{\text{nuc}} \uparrow$
 cf. L_g/L \Downarrow
 $\Delta T \uparrow$
 \Downarrow
 cf. M_{cc}/M convection

\uparrow \leftarrow ^{12}C used up \Rightarrow more contraction, $L \uparrow, \rho_c \uparrow, T_c \uparrow$
 $\epsilon_{\text{nuc}} \Rightarrow$ grav. contraction retarded temporarily
 ρ_c, T_c leveled out
 Total $L \downarrow$ ($\because L_g$)



Evolution on the Main Sequence

Evolution on the Main Sequence

(H core burning)

Hydrogen depletion core

mass \uparrow $H \rightarrow He \Rightarrow \mu \uparrow$ increases

$$P_{\text{gas}} \propto \frac{1}{\mu} \cdot P_{\text{gas}} \downarrow$$

pressure not sufficient to support the core

\Rightarrow core contraction (v. slow)

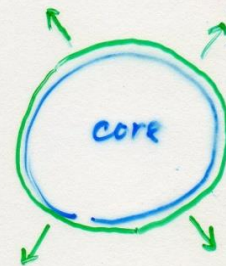
i.e. in equilibrium

$P_c \uparrow, T_c \uparrow$ \therefore even though $X_c \downarrow$

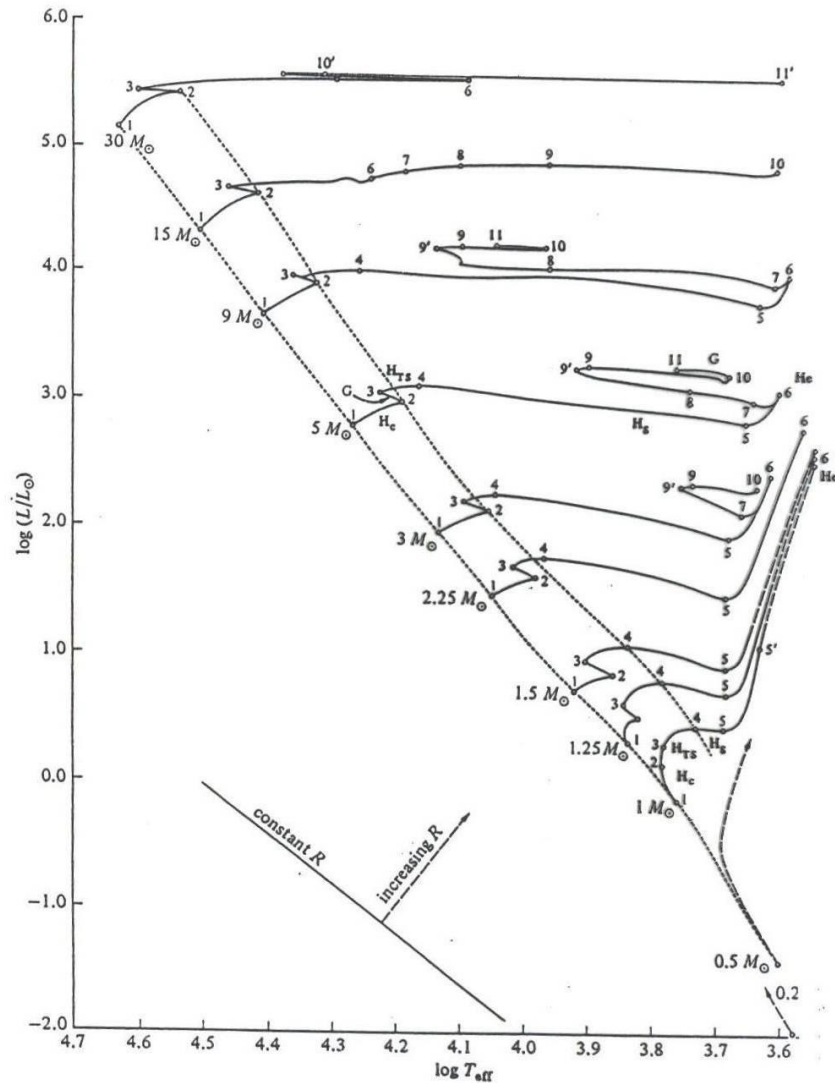
but $\epsilon \uparrow \Rightarrow L \uparrow$ of HR diagram

\Rightarrow overlying layers expand

L_r in a thin shell $\Rightarrow T_{\text{eff}} \downarrow$



\rightarrow (Hydrogen shell burning)



H_c : H core burning
 H_{TS} : H thick shell
 H_s : H thin shell

Table 7-7 Evolutionary Times. The times, expressed in years, refer to intervals between the points in Fig. 7-25.* [Adapted from I. Iben, Jr., 1967 (327).]

MASS (M_{\odot})	INTERVAL				
	1-2	2-3	3-4	4-5	5-6
30	4.80 (6)	8.64 (4)	← ~ 1.0 (4) →		
15	1.010 (7)	2.270 (5)	← 7.55 (4) →		
9	2.144 (7)	6.053 (5)	9.113 (4)	1.477 (5)	6.552 (4)
5	6.547 (7)	2.173 (6)	1.372 (6)	7.532 (5)	4.857 (5)
3	2.212 (8)	1.042 (7)	1.033 (7)	4.505 (6)	4.238 (6)
2.25	4.802 (8)	1.647 (7)	3.696 (7)	1.310 (7)	3.829 (7)
1.5	1.553 (9)	8.10 (7)	3.490 (8)	1.049 (8)	≥ 2 (8)
1.25	2.803 (9)	1.824 (8)	1.045 (9)	1.463 (8)	≥ 4 (8)
1.0	7 (9)	2 (9)	1.20 (9)	1.57 (8)	≥ 1 (9)

MASS (M_{\odot})	INTERVAL				
	6-7	7-8	8-9	9-10 ^(a)	10 ^(a) -11 ^(a)
30	← 53.1 (4) →				1.3 (4)
15	7.17 (5)	6.20 (5)	1.9 (5)	3.5 (4)	
9	4.90 (5)	9.50 (4)	3.28 (6)	1.55 (5)	2.86 (4)
5	6.05 (6)	1.02 (6)	9.00 (6)	9.30 (5)	7.69 (4)
3	2.51 (7)		4.08 (7)	6.00 (6)	

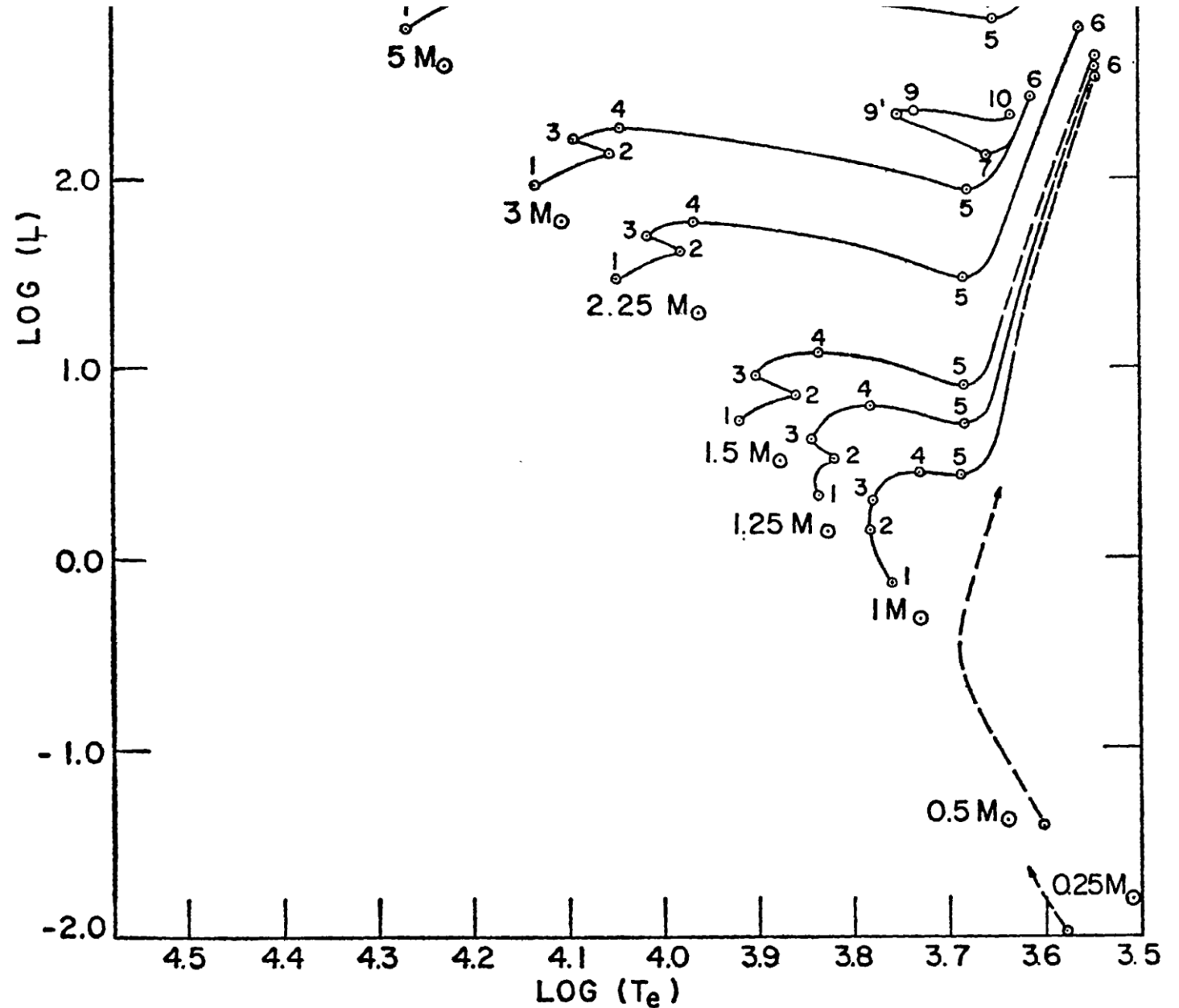
* A number in parentheses is the power of 10 by which an entry is to be multiplied.

Fig. 7-25 Evolutionary Tracks in the Hertzsprung-Russell Diagram. The mass of each star is given at the left of the track. The composition is $X = 0.708$, $Y = 0.272$, and $Z = 0.020$ for all masses except $30 M_{\odot}$, for which the composition is $X = 0.70$, $Y = 0.27$, $Z = 0.03$. Dashed portions of the curves are estimates. The letters along the tracks for $1 M_{\odot}$ and $5 M_{\odot}$ have the following significance: H_c = hydrogen-burning near the center; G = gravitational contraction of the entire star; H_{TS} = hydrogen-burning in a thick shell; H_s = hydrogen-burning near the center plus hydrogen-burning in a thin shell. The times required to reach the encircled points are given in Table 7-7.

The dotted lines indicate the boundaries of the main sequence. The line (lower left) shows the slope of a path along which the radius remains constant. The track for $15 M_{\odot}$ does not turn back as do the other tracks because the semi-convective zone was treated as fully convective [see R. Stothers and C.-W. Chin, 1968 (377)]. [Adapted from I. Iben, Jr., 1967 (327). The track for $30 M_{\odot}$ is given by R. Stothers, 1966 (333).]

As a star evolves off the MS
 $H_c \rightarrow H_{TS} \rightarrow H_s$

- 1-2 main sequence
- 2-3 overall contraction
- 3-4 H thick shell burning
- 5-6 H thin shell burning
- 6-7 red giant
- 7-10 core He burning
- 8-9 envelope contraction



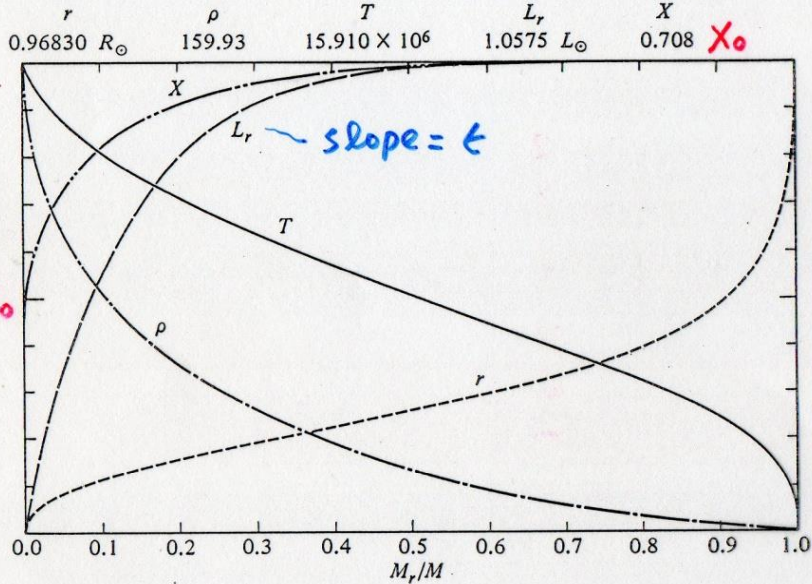


Fig. 7-10A A Model of Mass $1 M_{\odot}$ during the Main-Sequence Phase at Time $t = 4.26990 \times 10^9$ Years. Radius r , density ρ , temperature T , net luminosity L_r , and hydrogen abundance X are shown as functions of fractional mass M_r/M . The lower limit of the ordinate is zero for all variables. The upper limits, given in the figure, are the total radius R (units of $R_{\odot} = 6.96 \times 10^{10}$ cm), central density ρ_c (gm cm^{-3}), central temperature T_c in degrees Kelvin, total luminosity L (units of $L_{\odot} = 3.86 \times 10^{33}$ erg sec $^{-1}$), and initial hydrogen abundance $X = 0.708$. The central pressure (not shown) is 2.5186×10^{17} dyne cm $^{-2}$. The time t is measured from the initial model calculated for the pre-main-sequence phase (see Section 2). [Adapted from I. Iben, Jr., 1967 (326).]

Zero-age Main Sequence (ZAMS)
 \equiv homogeneous chemical composition

Termination of MS
 \equiv end of H burning at core

H depletion core

$X \approx 0, L_r \approx 0, \nabla T \approx 0$

$\Rightarrow \epsilon_{\text{nuc}}$ in a thin shell

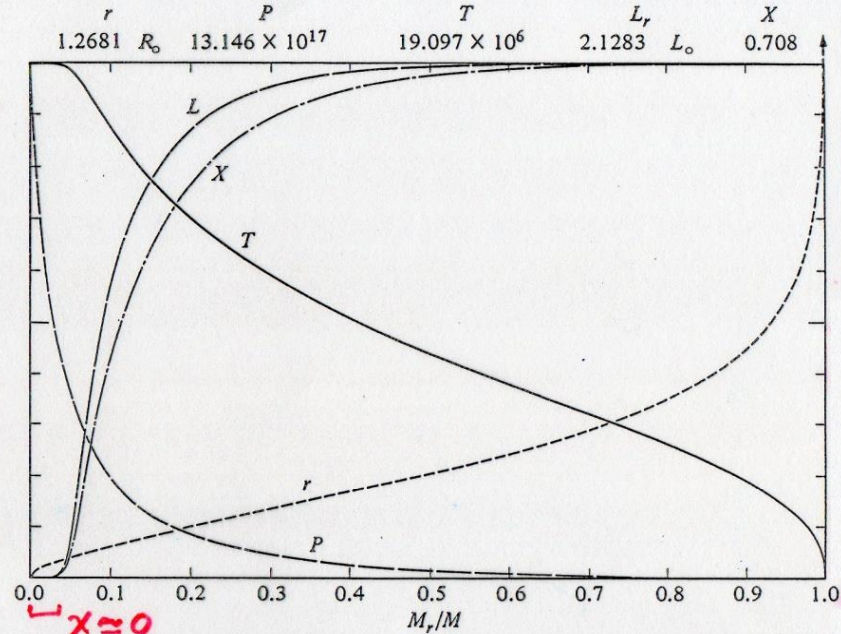


Fig. 7-10B A Model of Mass $1 M_{\odot}$ during the Main-Sequence Phase at Time $t = 9.20150 \times 10^9$ Years. Radius r , pressure P , temperature T , net luminosity L_r , and hydrogen abundance X are shown as functions of fractional mass M_r/M . The lower limit of the ordinate is zero for all variables. The upper limits, given in the figure, are 1.2681 R_{\odot} (with $R_{\odot} = 6.96 \times 10^{10}$ cm; however, the total radius is 1.3526 R_{\odot}), central pressure P_c (dyne cm $^{-2}$), central temperature T_c in degrees Kelvin, total luminosity L (units of $L_{\odot} = 3.86 \times 10^{33}$ erg sec $^{-1}$), and initial hydrogen abundance $X = 0.708$. The central density (not shown) is 1026.0 gm cm $^{-3}$. The time t is measured from the initial model calculated for the pre-main-sequence phase (see Section 2). [Adapted from I. Iben, Jr., 1967 (326).]

As τ goes on, $M_{\text{core}}^{\text{H}=0} \uparrow$, until $M_c \approx 0.1 M_{\odot}$

Schönberg-Chandrasekhar limit (1942) ApJ 96, 16
 maximum fraction of total mass maintainable within an isothermal core

1 M_{\odot} Stars on the Main Sequence

$4 H \rightarrow He$ $n \downarrow \rightarrow \rho \downarrow \rightarrow$ core contracts
(slowly)

$$\epsilon_{pp} \sim \rho X^2 T_c^4$$

H depletion $X \downarrow$ but $T \uparrow, \rho \uparrow$

$$\therefore \epsilon \uparrow \Rightarrow L \uparrow$$

(Faint distant sun dilemma)

\rightarrow envelope $R \uparrow$

H depleted core $L_r = 0$, but ϵ_{nuc} in a thick shell around the core

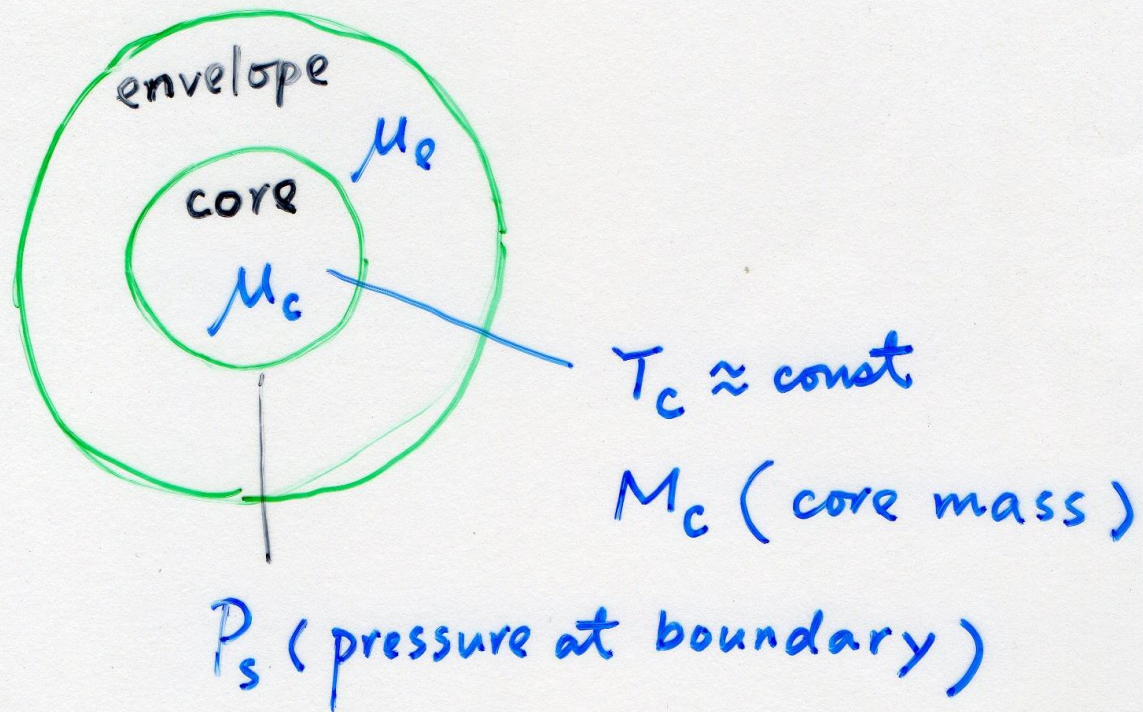
$$L_{TS} > L_{core}(MS)$$

$$\Rightarrow L \uparrow \rightarrow R \uparrow \Rightarrow T_{eff} \downarrow$$

Point 4 \equiv End of MS

Star \rightarrow subgiant branch

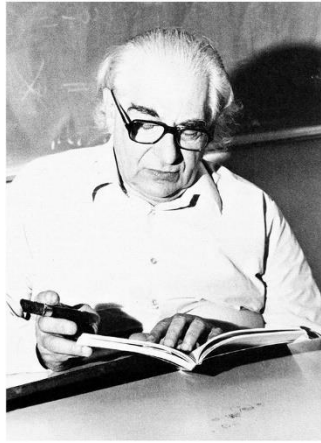
until M_{SC} is reached
($\sim 8-10\%$)



$T_c \approx \text{const}$

M_c (core mass)

P_s (pressure at boundary)



Mário Schenberg
(1914 Brazil – 1980)



Subrahmanyan Chandrasekhar
(1910 India – 1995 USA)

The Schönberg-Chandrasekhar limit
--- the maximum mass of a fusion-less stellar core that can support against gravitational collapse

THE ASTROPHYSICAL JOURNAL

AN INTERNATIONAL REVIEW OF SPECTROSCOPY AND
ASTRONOMICAL PHYSICS

VOLUME 96

SEPTEMBER 1942

NUMBER 2

ON THE EVOLUTION OF THE MAIN-SEQUENCE STARS

M. ŠCHÖNBERG¹ AND S. CHANDRASEKHAR

ABSTRACT

The evolution of the stars on the main sequence consequent to the gradual burning of the hydrogen in the central regions is examined. It is shown that, as a result of the decrease in the hydrogen content in these regions, the convective core (normally present in a star) eventually gives place to an isothermal core. It is further shown that there is an upper limit (~ 10 per cent) to the fraction of the total mass of hydrogen which can thus be exhausted. Some further remarks on what is to be expected beyond this point are also made.

$$\frac{M_c}{M} \approx 0.37 \left(\frac{\mu_e}{\mu_c} \right)^2 \left(\sim 10-15\% \text{ in reality} \right)$$

Take ionized H in env; pure He in core $\mu = 1.34$
 $\mu = 0.61$
 $M_c \sim 8-9\% M$ $\mu_c \sim 2 \mu_e$

Beech 1988

(Point 4, 5) shortly after the MS

ϵ_{nuc} in a thin shell

$L_{\gamma} \uparrow \uparrow$ between 13% - 20%

core experiences gravitational contraction $L_g > 0$

$\Rightarrow \nabla T$

$\rho_c \rightarrow 1.5 \times 10^4 \text{ g cm}^{-3}$, P_{deg} important ($= 0.46 P_{\text{total}}$)

convection beyond 63% M \rightarrow mixing $\rightarrow X \approx \text{const}$

(Point 5') $P_{deg} = 76\% P_{total}$

$T_{shell} \uparrow\uparrow$ $\epsilon_{CN} > \epsilon_{pp} \Rightarrow R \uparrow\uparrow, T_{eff} \downarrow\downarrow$

$K \uparrow$ in envelope \rightarrow convection for outer

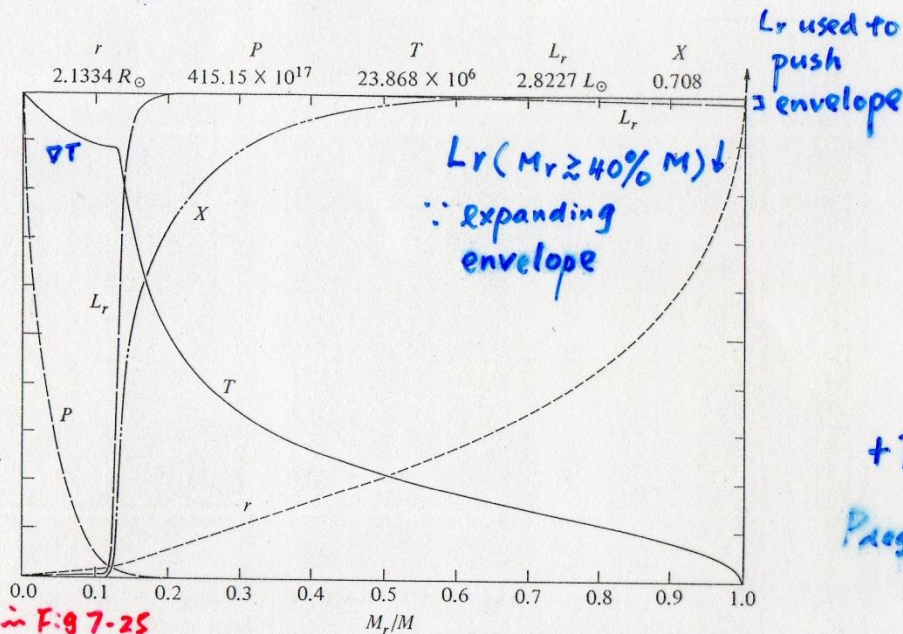
$71 \approx 71\% M$

$X \approx \text{const}$ for outer $29\% M$
beyond

∇T in core \leftarrow grav. contraction

$\rho_c = 1.5 \times 10^4 \text{ g cm}^{-3} \Rightarrow P_{\text{deg}} = 46\% \text{ of } P_{\text{total}}$

ϵ in a shell \quad so $M_c > M_{\text{sc}}$ OK



4-5 in Fig 7-25

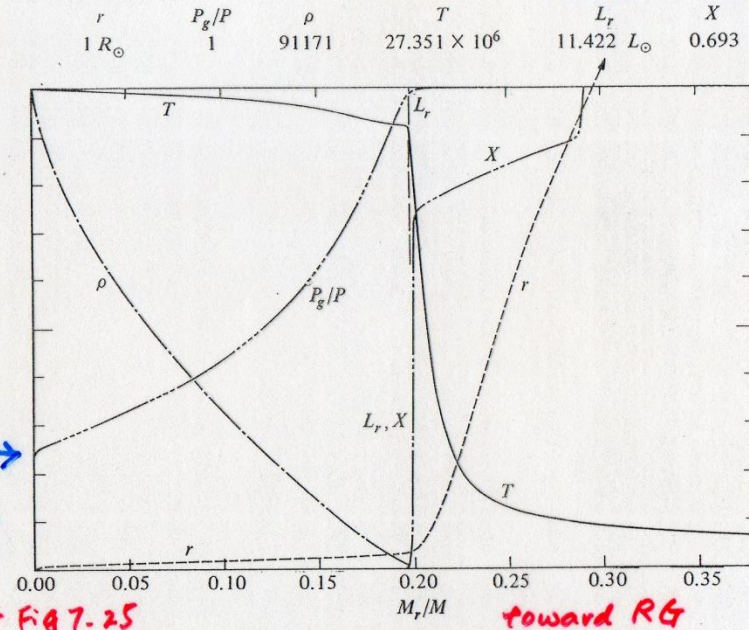
Fig. 7-26A A Model of Mass $1 M_{\odot}$ Shortly after Leaving the Main Sequence, at $t = 10.3059 \times 10^9$ Years. Radius r , pressure P , temperature T , net luminosity L_r , and hydrogen abundance X are shown as functions of fractional mass M_r/M . The lower limit of the ordinate is zero for all variables. The upper limits, given in the figure, are $2.1334 R_{\odot}$ (with $R_{\odot} = 6.96 \times 10^{10}$ cm; however, the total radius is $2.2179 R_{\odot}$), central pressure P_c (dyne cm^{-2}), central temperature T_c ($^{\circ}\text{K}$), total luminosity L (units of $L_{\odot} = 3.86 \times 10^{33}$ erg sec^{-1}), and initial hydrogen abundance $X = 0.708$. The central density (not shown) is $15,214 \text{ gm cm}^{-3}$. The time is measured from the initial model calculated for the pre-main-sequence phase (see Section 2). [Adapted from I. Iben, Jr., 1967 (326).]

$X \approx \text{const} > 63\% M \quad \therefore$ convection (mixing)

$\rho_c \sim 10^5 \text{ g cm}^{-3} \quad \frac{P_{\text{deg}}}{P_{\text{tot}}} \sim 46\%$

$T_s \uparrow \uparrow \Rightarrow \epsilon_{\text{CN}} > \epsilon_{\text{PP}}$

$X (M > 30\%) \approx \text{const} \therefore$ convection



+ $P_{\text{deg}} \rightarrow$
 $P_{\text{deg}} = 0.76 P$

5' in Fig 7-25

Fig. 7-26B A Model of Mass $1 M_{\odot}$ during the Subgiant Stage at $t = 10.8747 \times 10^9$ Years. Radius r , ratio P_g/P of gas pressure computed from the perfect gas law to the actual pressure with degeneracy included, temperature T , net luminosity L_r , and hydrogen abundance X are shown as functions of fractional mass M_r/M in the range 0 to 0.38. The distribution of L_r is a step function rising from zero to maximum scale with the initial rise in X . The lower limit of the ordinate is zero for all variables. The upper limits, given in the figure, are $1 R_{\odot}$ (with $R_{\odot} = 6.96 \times 10^{10}$ cm; however, the total radius is $6.1784 R_{\odot}$), unity for the ratio of pressures, central density ρ_c (gm cm^{-3}), central temperature T_c ($^{\circ}\text{K}$), total luminosity L (units of $L_{\odot} = 3.86 \times 10^{33}$ erg sec^{-1}), and hydrogen abundance $X = 0.693$. The central pressure (not shown) is $6552.2 \text{ dyne cm}^{-2}$. The time is measured from the initial model calculated for the pre-main-sequence phase (see Section 2). [Adapted from I. Iben, Jr., 1967 (326).]

Envelope expands and cools

Present Sun

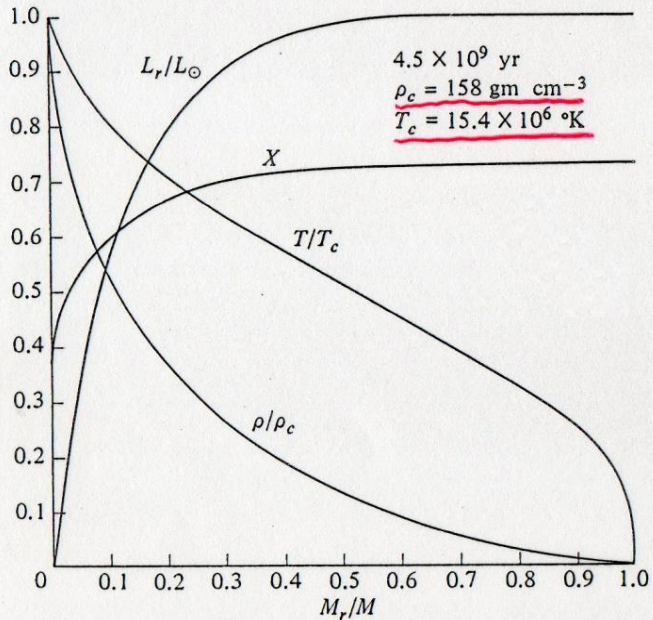


Fig. 7-11A A Model Solar Interior. Density relative to the central density ρ/ρ_c , temperature relative to central temperature T/T_c , net luminosity relative to total luminosity L_r/L_\odot , and hydrogen abundance X are shown as functions of fractional mass M_r/M . The chemical composition is $X = 0.730$, $Y = 0.245$, and $Z = 0.025$. The age is 4.5×10^9 years. [After S. Torres-Peimbert, E. Simpson, and R. K. Ulrich, 1969 (329).]

$X_c = 0.376$

Sun on the main sequence

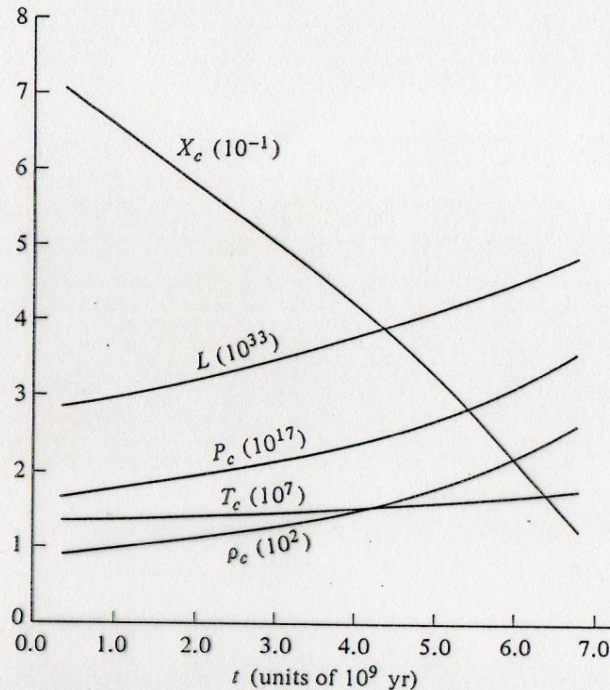


Fig. 7-11B The Evolution of the Sun during 7 Billion Years. Total luminosity L and central values of pressure P_c , temperature T_c , density ρ_c , and hydrogen abundance X_c are shown as functions of time t , which is measured from the initial (homogeneous) state for which the composition is $X = 0.730$, $Y = 0.245$, and $Z = 0.025$. The power of ten by which each value must be multiplied is indicated in parentheses. The values of P_c , ρ_c , and L are expressed in cgs units, and T_c is expressed in degrees Kelvin. [After S. Torres-Peimbert, E. Simpson, and R. K. Ulrich, 1969 (329).]

$P_{deg} \sim 0.017 P_{total}$ at ZAMS

0.075

9.2×10^9 yr

(Fig 7-10B)

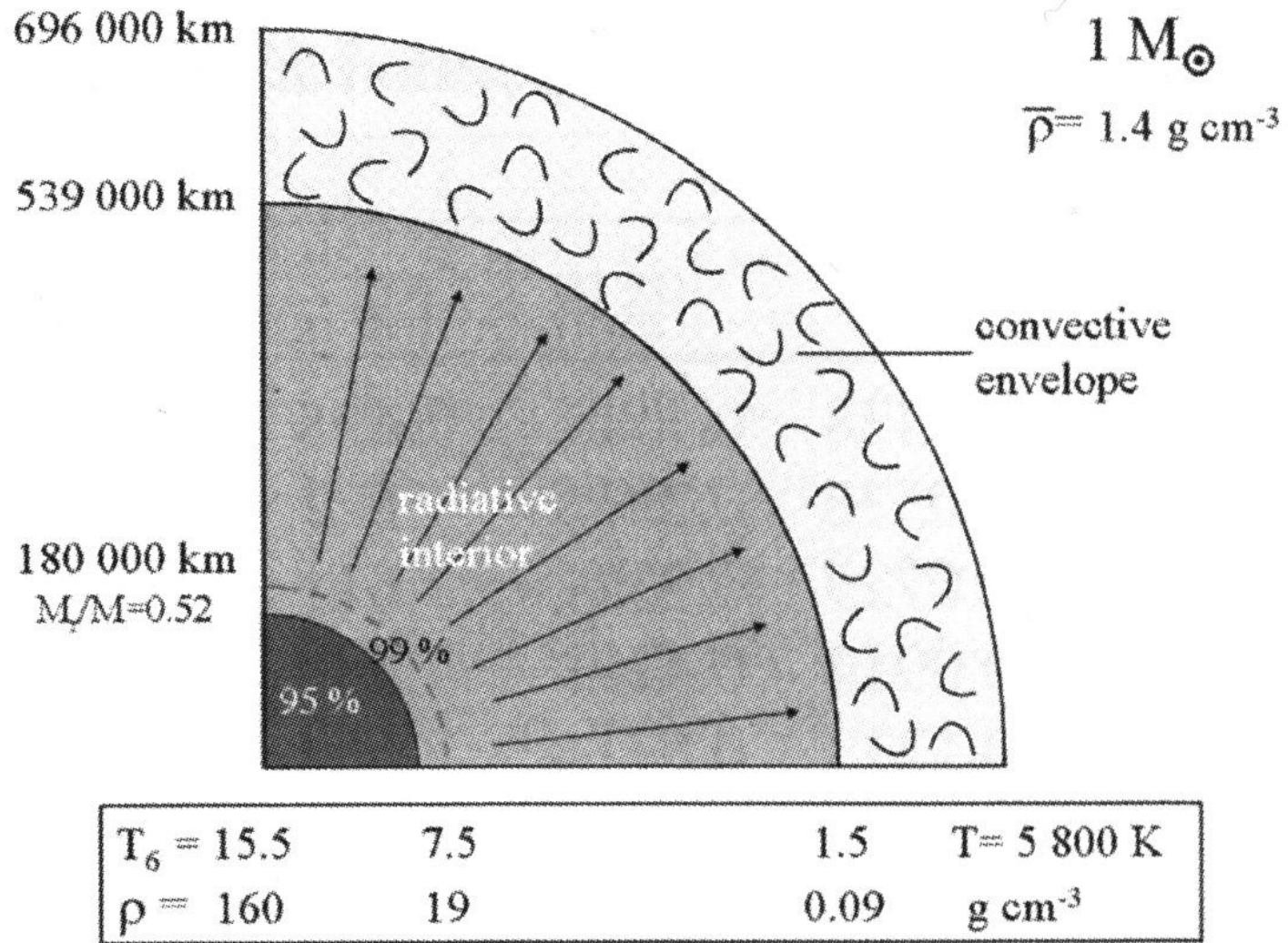
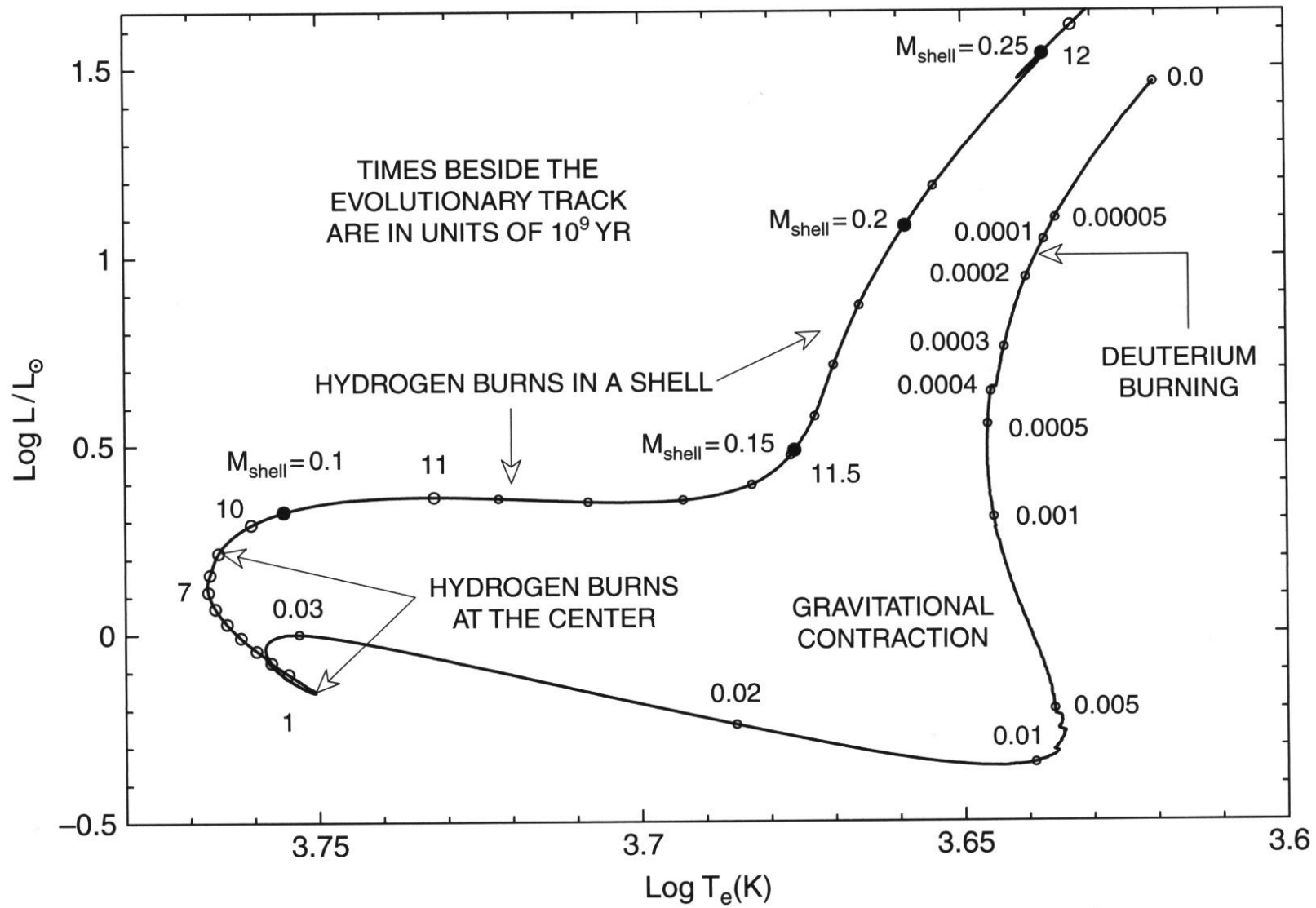


Figure 3.2. The present structure of the Sun. The physical parameters are indicated in the figure. The temperature T_6 is in million K. *From Maeder (2009).*



Evolutionary track of a $1M_{\odot}$ model ($Z = 0.015, Y = 0.275$) during gravitational contraction and central and shell hydrogen-burning phases

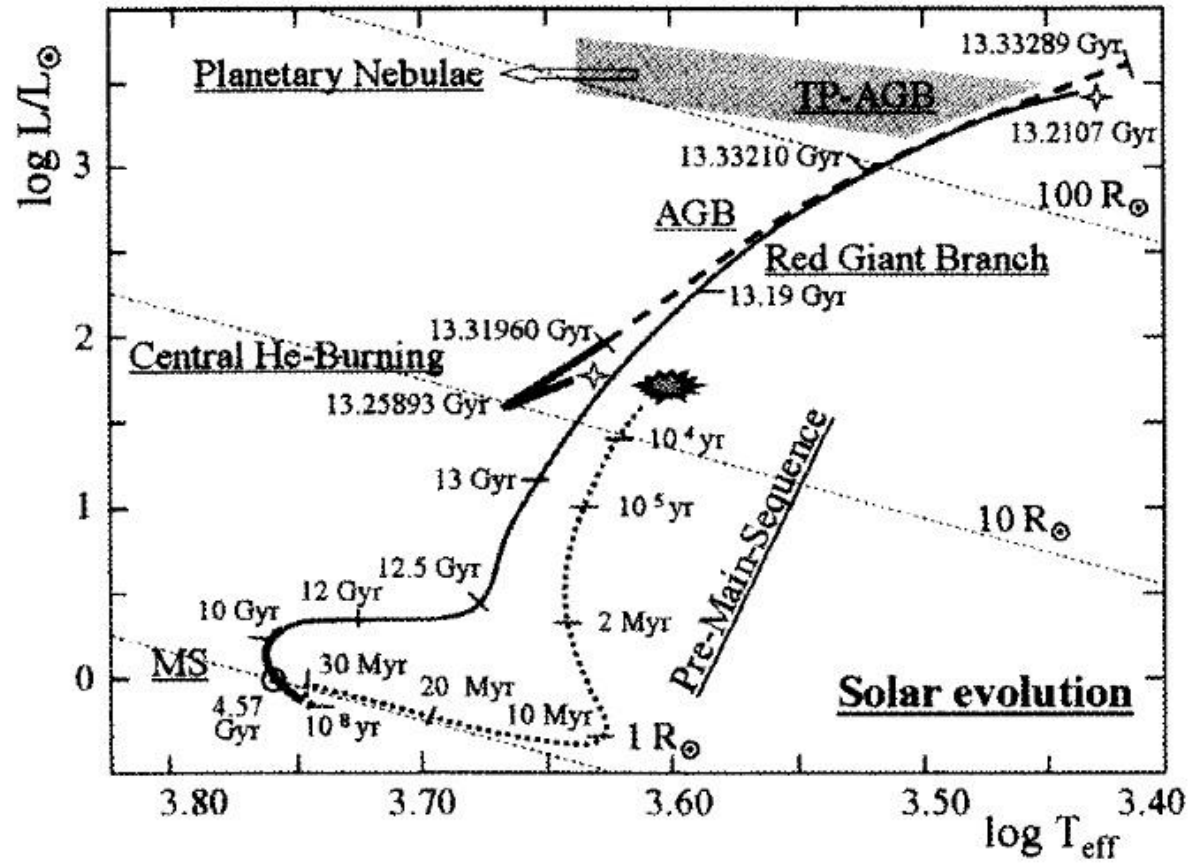


Figure 3.1. The evolution of the Sun. The evolution track of a solar-mass star is shown in the HR diagram from its formation to its death as a planetary nebula. Time is indicated at different steps along the track. The two 4-branch stars correspond to the helium flash and to the subsequent rapid rearrangement of the structure of the star. *From Maeder (2009), data from Corinne Charbonnel.*

Main Sequence Phase = core H burning

Evidence of thermonuclear reactions at a star's center, i.e., stellar evolution

- (solar) neutrinos

- heavy elements in evolved stars

(isotope ratios \neq YSOs)

'dredge-up' \leftarrow convective zone

to bring processed materials to surface

- Stars "disappear", e.g., supernovae

$M \uparrow \Rightarrow$ smaller outer convective zone

For the Sun, convective zone only 2% solar mass below the photosphere

$M \lesssim 0.3 M_{\odot}$
star fully convective

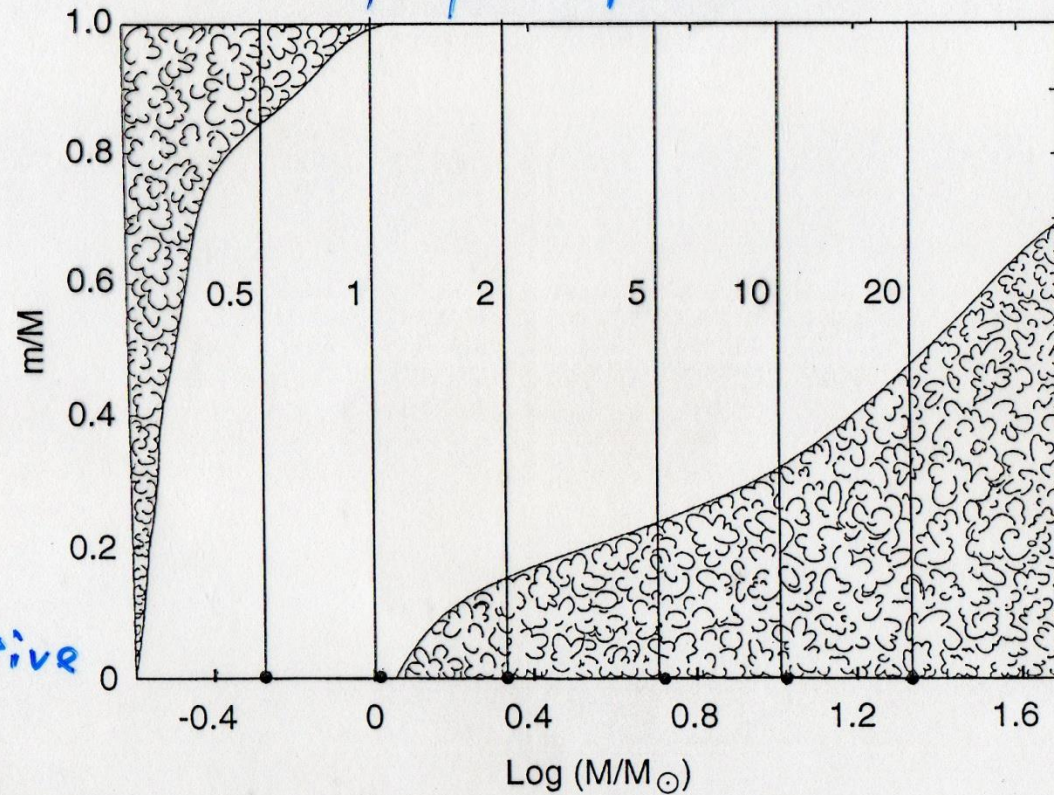
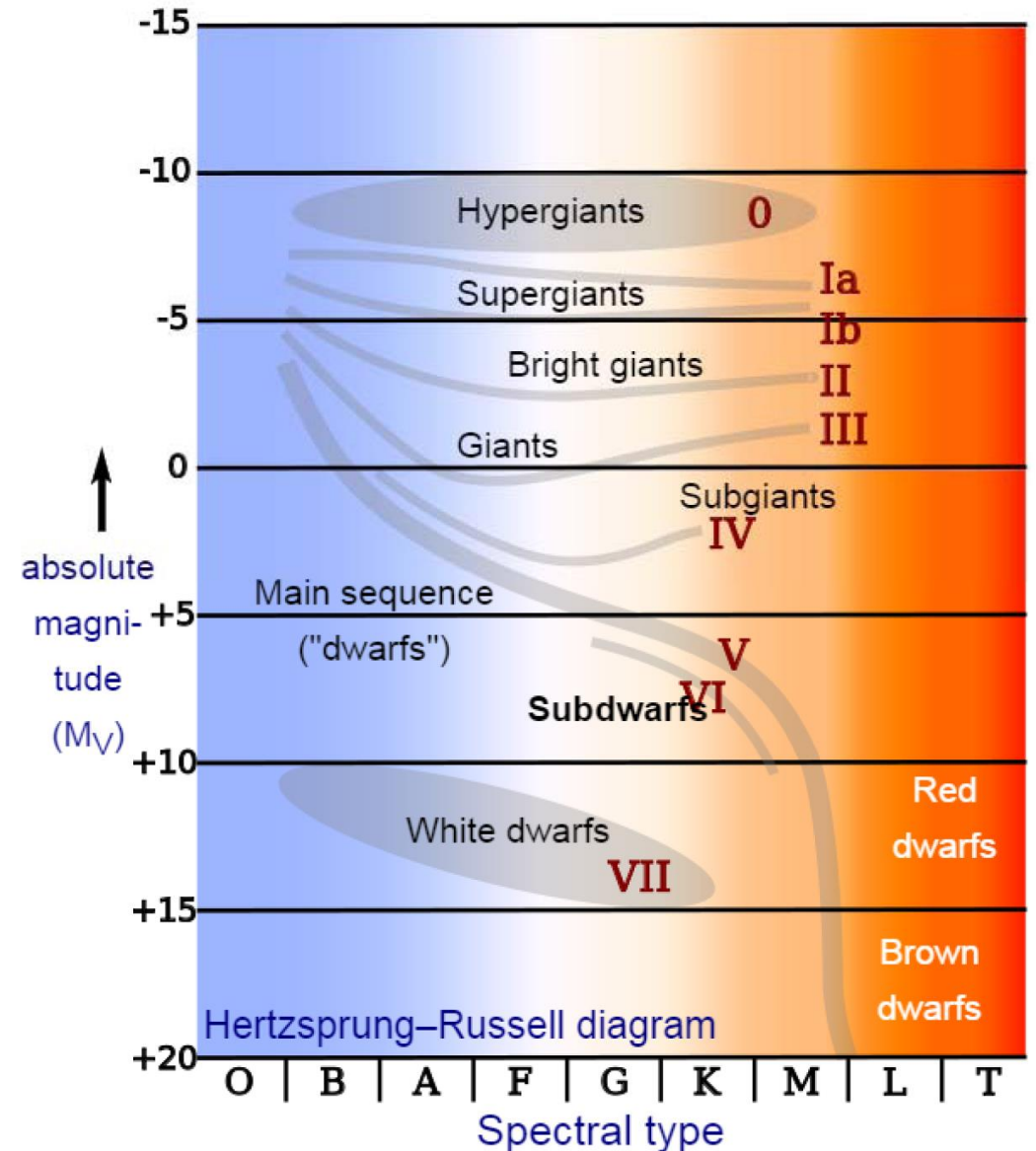


Figure 8.4 The extent of convective zones (shaded areas) in main-sequence star models as a function of the stellar mass [adapted from R. Kippenhahn & A. Weigert (1990), *Stellar Structure and Evolution*, Springer-Verlag].

Subdwarfs: The Pop II Main Sequence

- ◆ Luminosity class VI
- ◆ 1.5 to 2 mag fainter than a Pop I MS stars of the same spectral type
- ◆ Low metallicity \rightarrow low opacity \rightarrow (UV excess) \rightarrow low radiation pressure, so smaller, hotter for the same stellar mass



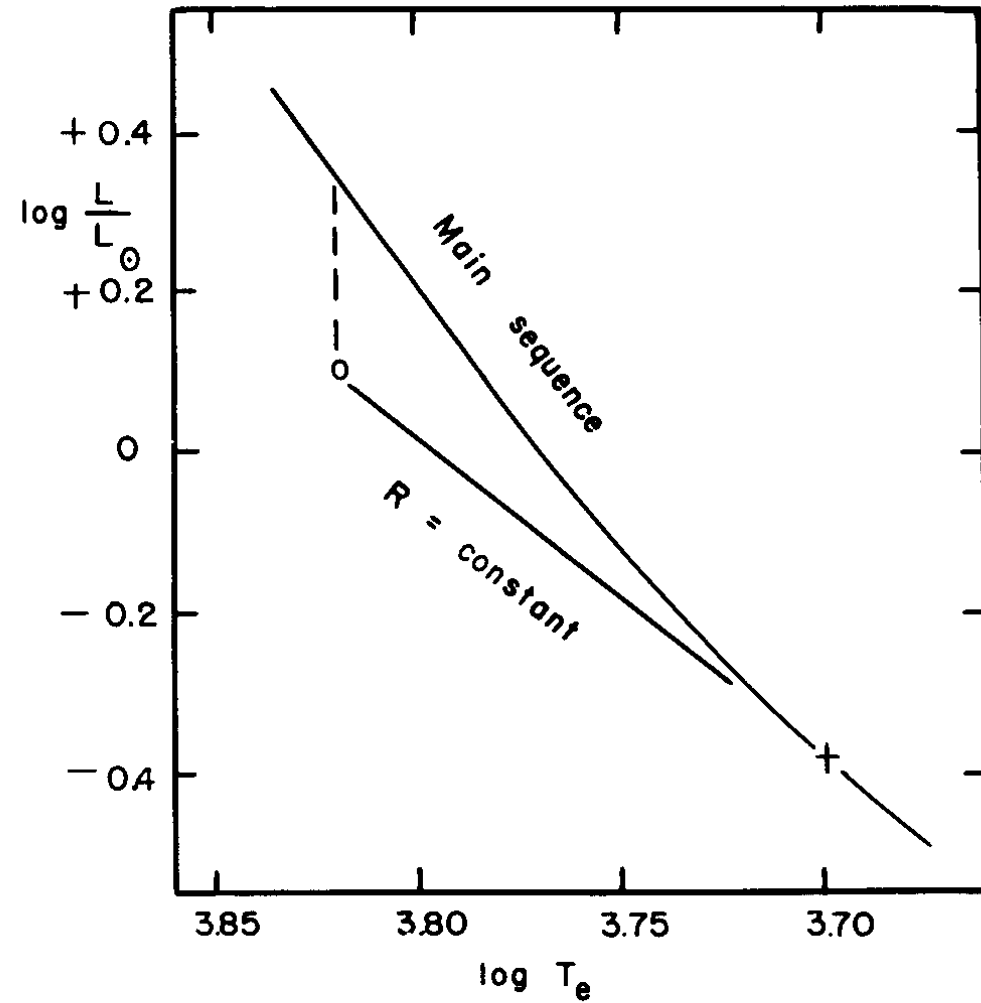


Fig. 17.1. Relation of subdwarfs to the main-sequence in the Hertzsprung-Russell diagram.